4. RESULTS AND DISCUSSION

4.1 SprX, highly conserved small RNA expresses in *S. aureus*

Small RNA SprX is encoded from the pathogenicity island and was discovered a decade ago in *Staphylococcus aureus* strain N315. SprX is highly conserved among the *S. aureus* and located in many *S. aureus* phages genomes such as 80α, tp310-3, 52-A, phiNM (Bohn *et al*., 2010). We have previously reported the role of SprX in virulence regulation in *S. aureus* Newman (Kathirvel *et al*., 2016). *S. aureus* Newman strain used in this study is a human clinical isolate containing the four prophages φNM1-4 which encode for various virulence genes and sRNAs, that play role in *S. aureus* survival and are also found to be significant contributors to the evolution of the staphylococcal genome (Baba *et al*., 2008). Small RNAs encoded from the four pathogenicity islands are listed in Table 9. Most strains of *S. aureus* contain a single copy of SprX such as N315 and MW2 whereas Newman contains three copies of SprX with a difference of 6 nt. Three different copies of SprX, namely SprX1, SprX2 and SprX3, encoded from different prophages, φNM3, φNM1 and φNM4 respectively, were identified from the *in silico* analysis of the genomic location in *S. aureus* (Table 9). *S. aureus* strain N315 and MW2 which harbor a single copy of SprX show 97 % and 99 % sequence similarity respectively with SprX1 copy encoded from φNM3. Absence of other pathogenicity islands φNM1, φNM2 and φNM4 in N315 and MW2 strains (Baba *et al*., 2008) explains the varying number of SprX copies encoded by different strains which in turn influences the *S. aureus* pathogenicity.

4.2 Construction of a modified strain of SprX

The present study is focused on the analysis of functional role of sRNA SprX in the regulation of virulence of *Staphylococcus aureus* strain Newman. A SprX overexpressing strain pMN*sprX*, previously generated in the lab (Kathirvel *et al*., 2016) was used to analyze the effect of SprX on the proteomic profile of *S. aureus* Newman. The *sprX* knockdown strain was constructed by cloning in pCN40, the antisense *sprX* containing an antisense promoter (at the 3′ end of *sprX* gene) and excluding the native *sprX* promoter (Figure 12). The cloned knockdown SprX plasmid was passed through *E. coli* DC10B strain and electroporated into *S. aureus* Newman. Attempts were also made for the construction of disruption strain of *sprX* using pMAD plasmid. However successful genomic integration was not obtained.

Table 9: sRNAs expressed form the pathogenicity island in *S. aureus* Newman

sRNA	Start	Stop	coding strand
φNM1 encoded sRNA			
srn_9349	1980012	1980322	+
SprX2	1980518	1980666	-
srn_9660	2017588	2017972	+
srn_9670	2018982	2019366	+
srn_9671	2019068	2019159	-
srn_9680	2019373	2019729	+
srn_9681	2019391	2019458	-
φNM2 encoded sRNA			
srn_9650	1103685	1104067	-
srn_3850_Teg123	1104388	1104422	-
srn_9342	1141253	1141502	+
srn_9343	1141515	1141653	-
srn_9344	1141525	1141656	+
srn_9345	1141676	1141990	+
srn_9346	1141677	1141847	-
φNM3 encoded sRNA			
srn_3790_sRNA301	2088540	2089074	+
srn_3800_sprD	2089939	2090083	-
srn_3810_Teg124	2090144	2090219	-
SprX1	2091551	2091700	-
srn_3830_sprF1	2093787	2093924	+
srn_3840_sprG1	2093788	2094154	-
srn_9430_sRNA312	2106751	2106928	+
srn_3850.1_Teg123	2124802	2124851	+
srn_3860_sRNA315	2130249	2130370	+
φNM4 encoded sRNA			
srn_0780_Sau6733	318216	318295	+
srn_0790_Sau6657	318970	319060	-
srn_9360_sRNA293	337754	338024	+
SprX3	363398	363546	+
srn_9640	363785	364009	-

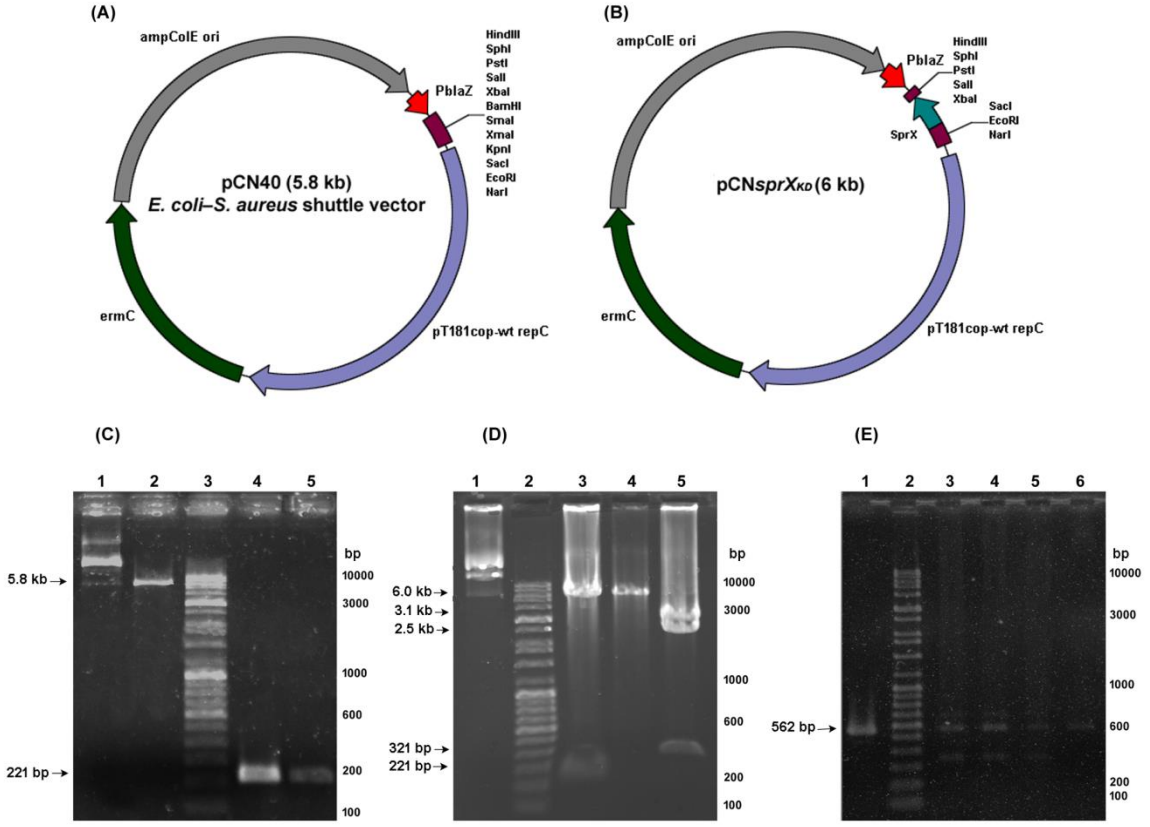

Figure 12: Construction of *sprX* knockdown strain

(A) Map of pCN40 plasmid containing the *Pbla* promoter used in this study. (B) Map of pCN*sprX*$_{KD}$ plasmid containing *sprX* cloned in antisense orientation. (C) Restriction digestion of pCN40 and *sprX* antisense PCR product. Lane-1: Undigested pCN40 plasmid, Lane-2: BamH1-KpnI Digested pCN40, Lane-3: High Range Marker, Lane-4: BamH1-KpnI Digested *sprX* antisense PCR product, Lane-5: Undigested *sprX* antisense PCR product. (D) Restriction digestion and clone confirmation in *E. coli*: Lane-1: Undigested Plasmid, Lane-2: High Range Marker, Lane-3: Insert release using BamHI and KpnI, Lane-4: Linearization of cloned plasmid with BamHI, Lane-5: Insert cut and confirmation of orientation with NsiI. (E) Confirmation of *sprX* antisense plasmid in *S. aureus* Newman by PCR amplification using vector specific forward primer and insert specific reverse primer. Lane-1: Positive control *sprX* antisense plasmid from *E. coli* DC10B, Lane2: High range marker, Lane 3-6: Clone (PCR product).

4.3 Expression analysis of small RNA SprX in *S. aureus* Newman

S. aureus Newman strains containing *sprX* overexpression and knockdown plasmids were employed for expressing altered levels of SprX. *sprX* knockdown strain was preferred over knockout for this study as *S. aureus* Newman encodes three copies of SprX expressing from different pathogenicity islands. In overexpression strains, *sprX* expressed weakly from the vector borne promoter (Kathirvel *et al*., 2016), and the increased level of SprX resulted from the native promoter in the multicopy plasmid. The expression of SprX was verified by qRT-PCR in these modified strains at different time

points along the growth curve. The transcripts increased by 1.2 - 1.8 fold, from late exponential to stationary phase, in the overexpression (pMN*sprX*) strain, while the knockdown strain showed a significant down regulation by 0.3 - 0.6 fold during growth, compared to the control (Figure 13).

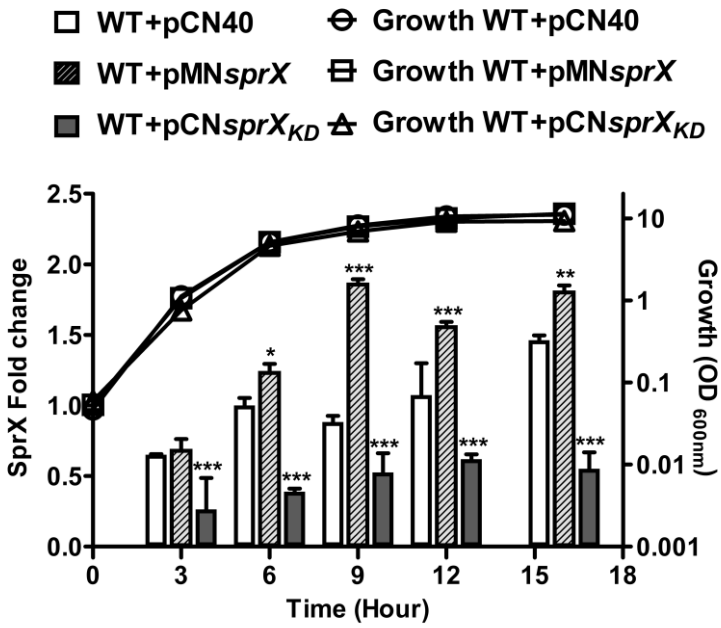

Figure 13: Expression of SprX in different strains in *S. aureus* Newman.

qRT-PCR of SprX expression in modified strains of *S. aureus* Newman, analyzed at different time points along growth. Data normalized with 5S rRNA and fold change was calculated as per the standard $\Delta\Delta^{Ct}$ method referred to the control (WT + pCN40) at 6 hour growth. The experiment was performed in triplicates; mean and standard deviation are plotted. * represents the statistically significant difference analyzed by two-way ANOVA at each time point compared with the control. *** ($P<0.001$) and ** ($P<0.01$).

4.4 SprX differentially regulates the protein profile in *S. aureus* Newman

Cell wall associated proteins, which are expressed maximally during the exponential growth phase, facilitate the adherence of *S. aureus* and interaction with diverse host surfaces, thereby contribute towards its pathogenicity. On the other hand, secretion of extracellular proteins at a later phase helps in dissemination and spread of infection. In order to identify additional targets regulated by SprX, a 2D-PAGE approach was used. Impact of the modified levels of SprX on extracellular and cell wall-associated proteins, was examined by two-dimensional gel electrophoresis. Proteins were extracted, purified and separated by two dimensional PAGE, using a pH gradient of 4-7 in the first

dimension (Figure 14). Differentially regulated proteins were excised from the gel and identified by LC–mass spectrometry (C-CAMP, Bangalore, India).

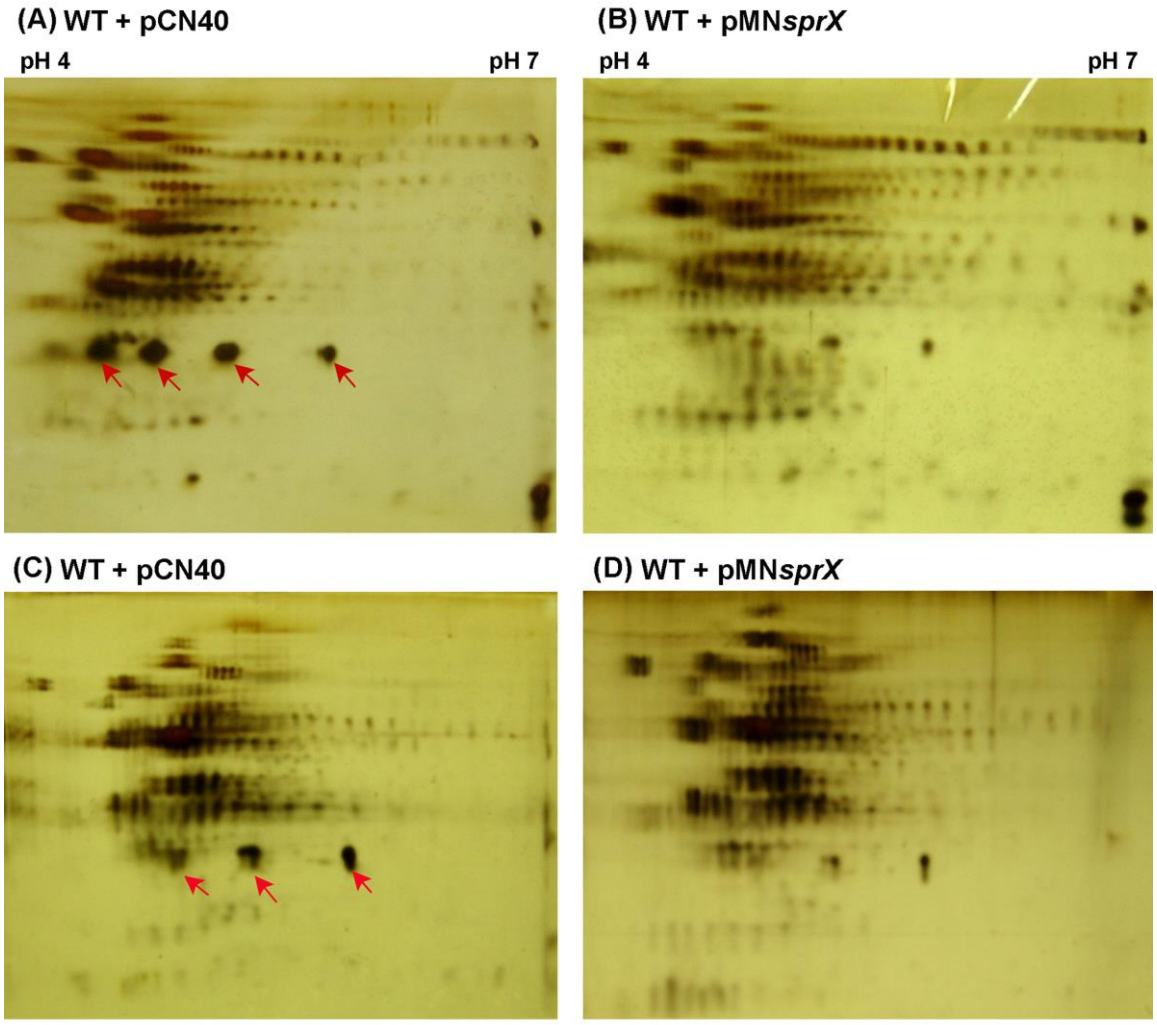

Figure 14: Differential protein profile of *S. aureus* Newman

Effect of altered levels of SprX on secreted (A & B) and cell wall associated proteins (C& D) was analyzed by 2D-gel electrophoresis. Proteins were separated based on pI using IEF on 4-7 pH IPG strips followed by separation of SDS-PAGE. Downregulated proteins marked in gel were identified as pI variant isomers (pI 4.5, 4.8, 5.1, and 5.7) of Immunodominant staphylococcal antigen A (IsaA).

A key protein that was found down-regulated under the overexpression of SprX was identified as Immunodominant staphylococcal Antigen A (IsaA). The four variant spots seen in line with the molecular weight of IsaA observed on gel indicated the different isoforms of this protein with pI variants (pI 4.5, 4.8, 5.1, and 5.7), as deduced from previous report (Cordwell *et al*., 2002). IsaA is a 29 kDa, profoundly antigenic, surface associated as well as secreted protein, that diminishes the biofilm formation in *S. aureus*

(Lorenz *et al*., 2000). It displays a lytic trans-glycosylase domain that promotes lysis and regulates clumping of cells, thereby playing a crucial role in staphylococcal growth and survival (Sakata *et al*., 2005; Sakata and Mukai, 2007).

4.5 SprX regulates the expression of IsaA

The effect of modified levels of SprX on the expression of the *isaA* transcript *was* analyzed by qRT-PCR at different time points along growth (Figure 15).

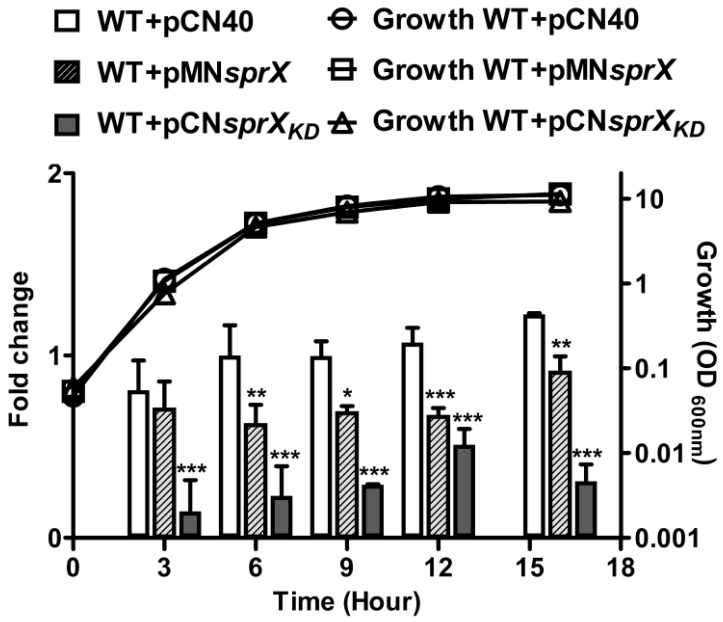

Figure 15: Influence of SprX on *isaA* expression in *S. aureus* Newman.

The expression of *isaA* transcripts under modified levels of SprX was monitored using qRT-PCR at different time points along growth. Significant down-regulation of *isaA* transcripts to 0.1 fold was observed in the *sprX* knockdown strain. A 0.6 - 0.9- fold reduction was observed in *sprX* overexpression strain. Data normalized with 5S rRNA and fold change was calculated as per standard $2^{-\Delta\Delta Ct}$ method referred to the control (WT + pCN40) at 6 h growth. The experiment was performed in triplicates; mean and standard deviations are plotted. * represents the statistically significant difference analyzed by two-way ANOVA and each time point is compared with the control. *** ($P<0.001$) and ** ($P<0.01$).

The expression of *isaA* transcript was significantly reduced to 0.1- 0.5 fold in *sprX* knockdown strain, A significant down-regulation of *isaA* to 0.6 - 0.9 fold was also observed in *sprX* overexpression strain, compared to the control, thus suggesting the involvement of other regulators in IsaA regulation. The downregulation of *isaA*, under *sprX* overexpression in our experiments can be elaborated by considering its complex

multifactorial regulation as rationalized in discussion in section 4.11 and Figures 24 and 25.

4.6 SprX binds at 3' coding region of *isaA* mRNA

Small RNA directly interacts with target mRNAs and modulates its expression through various mechanisms. The role of SprX was further studied by investigating the interaction between sRNA SprX and *isaA*, as a putative target. Potential interaction between sRNA SprX and *isaA* mRNA, analyzed *in silico* using IntaRNA program, indicated that 3′ coding region of *isaA* (C669 to G694) interacts with loop 2 of SprX between A36 to U61 nt (Figure 16A).

The above potential interaction between SprX and *isaA* mRNA was analyzed *in vitro* by gel mobility shift assays. SprX and *isaA* transcripts containing the predicted interaction regions were generated by *in vitro* transcription and gel-purified (Figure 16B). Unlabeled *isaA* mRNA was incubated in increasing molar ratios with DIG-labeled SprX. A weak duplex formation was detected between SprX and *isaA* mRNA, (Figure 16, C & D) which may reflect a feeble base pairing at the 3′ coding region of *isaA* mRNA and could additionally influence the expression of IsaA.

Small RNAs, binding at the 5' or 3' coding region, modulate mRNA degradation by interfering with the RNase mediated mRNA decay. Down regulation of *isaA* transcript in qRT-PCR and interaction of SprX with *isaA* mRNA suggest that SprX may modulate stability of mRNA by binding with the 3' region of *isaA* mRNA. Role of an additional regulator involved in the IsaA regulation is explained in the following study.

4.7 SprX modulates the expression of autolysins in *S. aureus* Newman

As described previously the effect of altered levels of SprX on secreted proteins and virulence factors of *S. aureus* identified the immunodominant antigen, IsaA, as one of the affected proteins in 2D gels. IsaA is a highly antigenic; cell wall associated and secreted autolysin with a lytic trans-glycosylase activity. Cell wall degrading autolytic activity of both, surface associated and secreted proteins, was analyzed under altered levels of SprX, in control (pCN40), *sprX* overexpression (pMN*sprX*) and *sprX* knockdown (pCN$sprX_{KD}$) strains of *S. aureus*, by renaturing SDS-PAGE, with *S. aureus* crude cell wall as the substrate. A differential regulation of multiple autolysins was observed as bands of cell wall hydrolysis amongst the major hydrolytic bands in the range, 29-120 kDa (Figure 17A). Significant reduction in autolysis was seen under

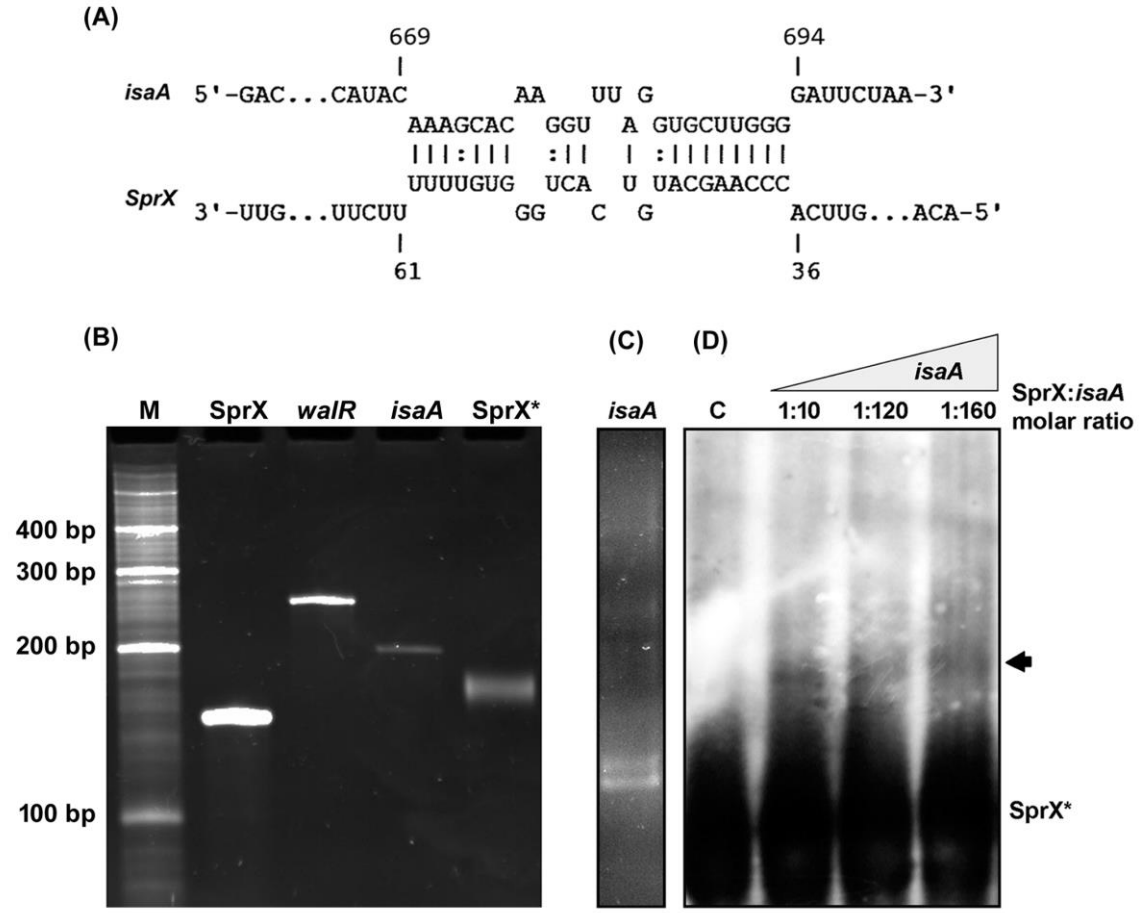

Figure 16 : Weak interaction of SprX with *isaA* mRNA

(A) *In silico* analysis of SprX-*isaA* mRNA interaction analyzed by IntaRNA. (B) Urea-PAGE of purified transcripts of unlabeled SprX (156 nt), *walR* (245 nt), *isaA* (199 nt) and DIG-labeled SprX* (156 nt) on 6 % - 6 M Urea-PAGE and stained with EtBr. (C) *isaA* transcript separated on 6% Native-PAGE stained with EtBr. (D) Gel mobility shift assay: 0.1 pmol of *in vitro* transcribed DIG-labeled SprX was incubated with increasing concentration of *isaA* mRNA (10X-160X). The complex was resolved on 6% Native-PAGE followed by transfer on Nylon membrane and detection by anti-DIG antibody. Arrow indicates the complex between SprX and *isaA* mRNA.

reduced expression of SprX in the knockdown strain, in the cell surface associated proteins, at bands of molecular weight around 96, 88, 72, 61, 51, and 28 kDa, and additionally in ~33 kDa, in secreted proteins. The autolytic bands were identified by comparing with the autolytic profile reported for AtlA and LytM under WalR induction (Dubrac *et al*., 2007). The major down regulated hydrolytic bands (~100 kDa, ~70 kDa and others) observed in zymography corresponded to the bifunctional autolysin AtlA and its processed intermediates, and the ~35 kDa band, corresponded to LytM.

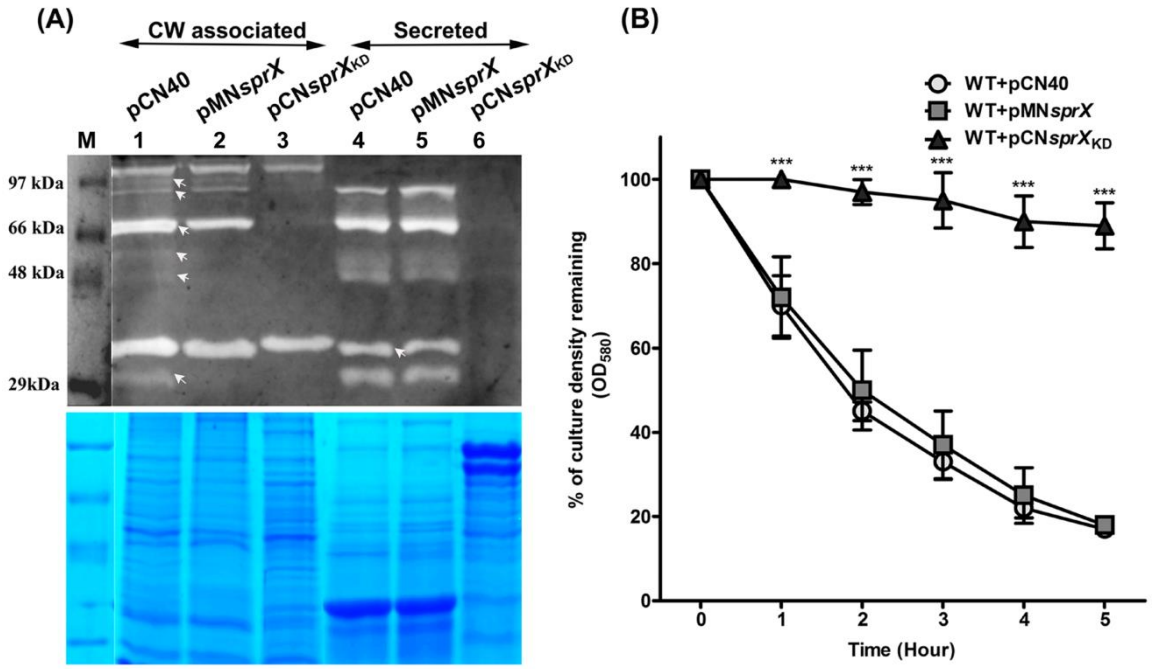

Figure 17 : SprX regulates the expression of autolysins

(A) Top: SDS-polyacrylamide gel containing isolated crude *S.aureus* cell wall was used to separate *S.aureus* proteins. Cell wall associated and secreted proteins were separately prepared and loaded on this gel. Activity of autolysins in these proteins was monitored as colorless bands. Lanes 1-3 cell wall associated proteins and lanes 4-6 secreted proteins. Inset arrows indicate down regulated autolysins under altered SprX levels. Bottom: Coomassie blue stained loading control. (B) Triton X-100-induced whole cell autolysis assay in strains expressing altered levels of SprX. (WT + pCN40)-control, (WT + pMN*sprX*)-overexpression and (WT + pCN$sprX_{KD}$)-knockdown strains of *S. aureus* Newman. Autolysis was analyzed in 0.1% Triton X-100 by measuring the change in optical density at a wavelength of 580 nm and calculated as relative percentage of autolysis. The experiment was done in triplicates; mean and standard deviations are plotted. * represents the statistically significant difference analyzed by two-way ANOVA and each time point compared with control (WT + pCN40). *** ($P<0.001$).

S. aureus expresses many cell wall-associated and secreted autolysins; yet the most prominent autolysin that it expresses is AtlA (138 kDa), a bifunctional protein with amidase (AM) and a glucosaminidase (GL) domain. Endo-β-*N*-acetylglucosaminidase (GL, 51 kDa) and *N*-acetyl muramyl-L-alanine amidase (AM, 62 kDa) are proteolytic products of bifunctional autolysin AtlA and play an important role in dispersing cell clusters of *S. aureus*. Cells which lacks the GL and AM protein in supernatant, grow in large clusters (Bose *et al.*, 2012; Sugai *et al.*, 1995). Manifestation of altered phenotypes, under altered levels of SprX, has been investigated.

4.8 *sprX* knockdown, an autolysin deficient strain, exhibits altered phenotypes

The altered level of autolysins in the knockdown strain was endorsed by Triton X-100-induced autolysis assay during growth. Triton X-100 removes the inhibitor of endogenous autolysin, lipoteichoic acid, and induces the autolysis in *S. aureus* (Raychaudhuri and Chatterjee, 1985). Exponentially grown cells (OD_{600}~1) were incubated with 0.1 % Triton X-100, and cell lysis was measured. As shown in Figure 17B, the control and *sprX* overexpression strains showed nearly 80 % lysis in 5 hours whereas the knockdown strain exhibited significantly higher resistance to Triton X-100-induced lysis, with only 10 % lysis occurring in 5 hours.

S. aureus strains, defective in autolysin production, are reported to have impaired cell division leading to high cell clustering (Delauné *et al.*, 2012; Dubrac *et al.*, 2007). Effect of SprX on cluster dispersion was initially analyzed by direct observation of growing cells on agarose pad under a 100X phase-contrast microscope. Well-separated cells were observed in the cases of control and *sprX* overexpression strains (Figure 18A and B) respectively. In contrast, an increased cell clustering was observed in the *sprX* knockdown strain (Figure 18C).

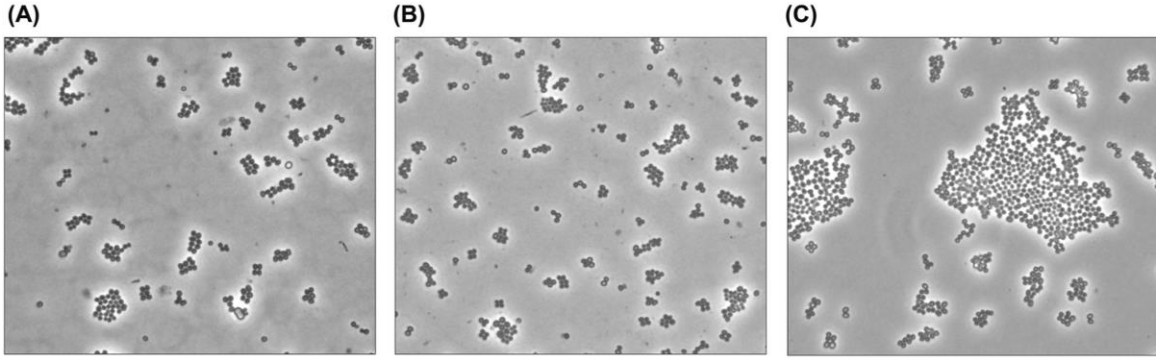

Figure 18**: Effect of SprX on cell clustering by phase-contrast microscopy**
Magnification-1000X (A) Control (WT + pCN40), (B) overexpression (WT + pMN*sprX*), (C) knockdown (WT + pCN$sprX_{KD}$). *sprX* knockdown strain exhibited higher cell clustering compared to the overexpression and control.

Influence of SprX on clustered cell phenotype as a consequence of autolysin deficiency was also analyzed by scanning electron microscopy. In agreement with the phase contrast, well-separated cells in small clusters were observed in the cases of both control and *sprX* overexpression strains (Figure 19A and B). In contrast, the *sprX* knockdown strain

(Figure 19C) manifested big clusters of 25-30 cells due to defective cell separation, establishing the significance of SprX in autolysin regulation.

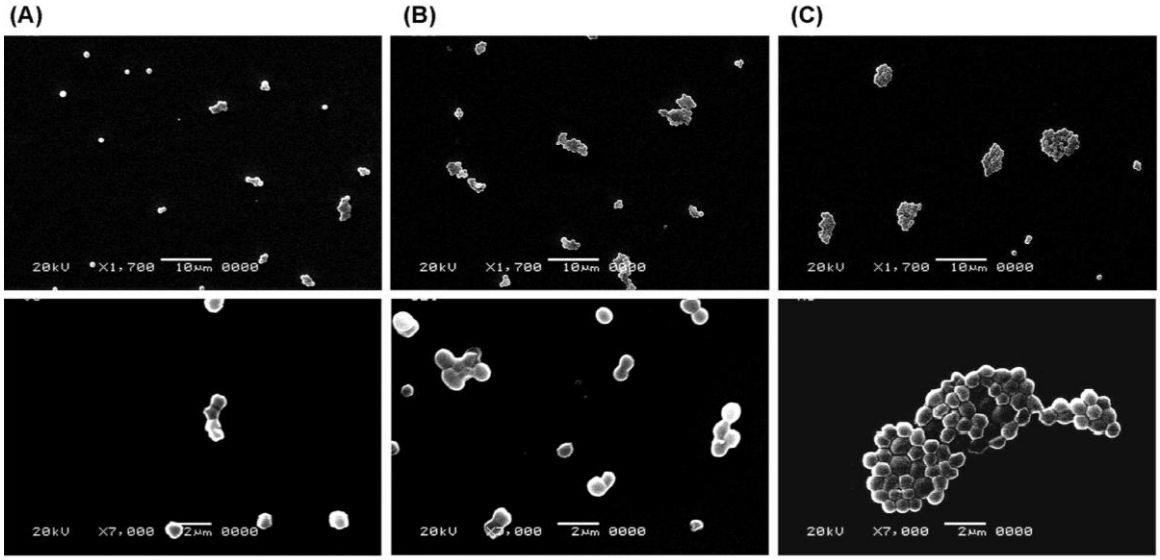

Figure 19: Effect of SprX on cell clustering by scanning electron microscopy
(A) Control (WT + pCN40), (B) overexpression (WT + pMN*sprX*), (C) knockdown (WT + pCN$sprX_{KD}$). Top: 1700x, scale bar 10 µm. Bottom: 7000x, scale bar 2 µm. *sprX* knockdown strain formed large clusters of 25-30 cells compared to the overexpression and control, where diplococci or very small clusters were observed.

The difference in cell clustering under altered levels of SprX was further analyzed by sedimentation assay by measuring the optical density from the top of the tube of cells statically incubated for up to 8 hours. The control and *sprX* overexpression strains displayed 20% reduction in turbidity whereas the *sprX* knockdown strain exhibited high settling with nearly 70 % reduction in turbidity (Figure 20A and B).

Autolysin mutants of *S. aureus* display reduced interaction and adherence with a diversity of substrates, and decreased accumulation of extracellular DNA, an important biofilm matrix molecule,(Bose *et al*., 2012) resulting in poor biofilm formation. The functional significance of autolysin on biofilm formation was confirmed by standard crystal violet-based microtiter plate assay. As seen in Figure 20C, 50 % reduction in biofilm formation was observed in *sprX* knockdown strain compared to the control whereas overexpression strain exhibited a 50% enhancement in biofilm formation. This result corroborates with the decreased expression of autolysins observed in zymography, high cellular clustering, and resistance to Triton X-100-induced lysis of *sprX* knockdown strain.

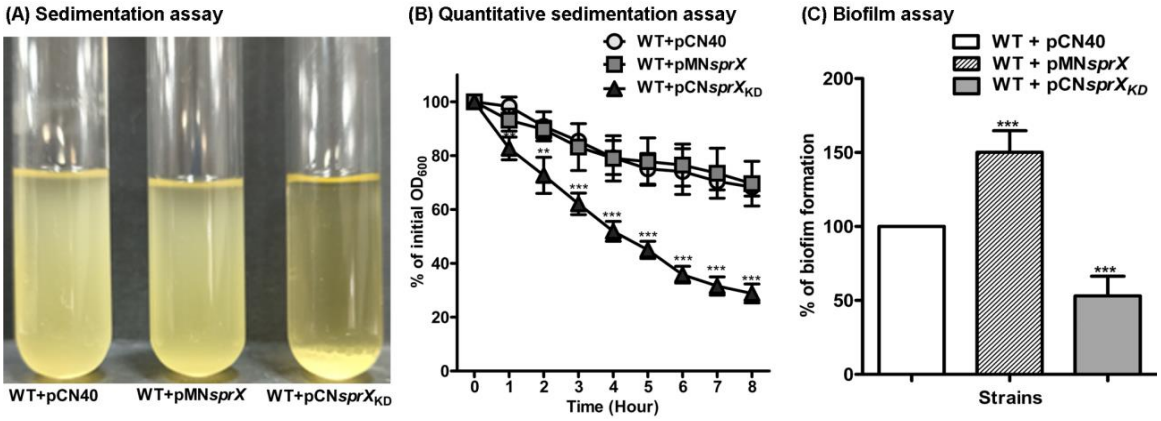

Figure 20: Influence of SprX on cell clustering and biofilm formation

(A) Sedimentation assay: 1 control (WT + pCN40), 2 overexpression (WT + pMN*sprX*) and 3 knockdown (WT + pCN$sprX_{KD}$). *sprX* knockdown strain displayed increased settling of cells compared to the control and overexpression strain. (B) Quantitative sedimentation assay in strains expressing altered levels of SprX. The difference in turbidity was measured at a wavelength of 600 nm from the top of the tube for 8 hours and data was reported as the percent of initial optical density of each strain. The experiment was performed in triplicates; mean and standard deviations are plotted. * represents the statistically significant difference analyzed by two-way ANOVA and each time point compared with the control (WT + pCN40). ** (P<0.01), *** (P<0.001). (C) Biofilm formation in control (WT + pCN40), overexpression (WT + pMN*sprX*) and knockdown (WT + pCN$sprX_{KD}$) stains of *S. aureus* Newman analyzed by crystal violet based microtiter plate assay. The amount of biofilm produced by each strain was calculated as a percentage of that produced in the control. Means and standard deviations of n=4 are plotted and the statistically significant difference was analyzed by one way- ANOVA. *** (P < 0.0001)

Autolysins have a major role in cell division and daughter cell separation. During the cell division the two daughter cells are interlinked through a narrow peripheral ring, and are resolved in the final step of cell division by major autolysin AtlA (Zhou *et al.*, 2015). Hence the reduced expression of genes involved in autolysin production leading to higher clustering is a well-known phenotype observed in *S. aureus*. AM and GL, localized at peripheral ring region during cell division, separate the daughter cells by resolving the peptidoglycan (Baba and Schneewind, 1998; Nega *et al.*, 2020; Yamada *et al.*, 1996). In addition to AtlA, IsaA which has a lytic transglycosylase activity and localized at the septal region of dividing cells, affects peptidoglycan turnover and division of the septum during daughter cell separation (Sakata *et al.*, 2005). Higher cell clustering phenotype observed in scanning electron microscopy indicates an impaired cell separation due to reduction in autolysin expression in *sprX* knockdown strain. Increased cell aggregation is a phenotype observed in IsaA, AltA and WalR mutants (Bose *et al.*, 2012; Dubrac *et al.*, 2007; Melanie R. Stapleton *et al.*, 2007).

Modification in cell wall metabolism is associated with a broad range of phenotypes such as sensitivity to antibiotics that target the cell wall, and a tendency in autolysin deficient strain to form aggregates in cell suspension. A decrease in WalR leads to increase in peptidoglycan cross-linking and glycan chain length (Dubrac *et al*., 2007) which influence the bacterial resistance to detergent induced lysis. Reduced expressions of autolysins enhanced the cell aggregation and resistance to Triton X-100-induced lysis of *sprX* knockdown strain. A defect in cell separation and sedimentation of cells in liquid culture was described in autolysin mutant stains (Foster *et al*., 2002; Kajimura *et al*., 2005). The increased settling of cells in sedimentation assay of *sprX* knockdown strain under reduced autolysin expression confirmed the SEM results.

Further, the downregulation of autolysin is reflected by its reduced biofilm phenotype. AtlA acts as an adhesin and is involved in the initial adherence of *S. aureus* during the biofilm formation. Release of extracellular DNA (eDNA) during cell lysis, mediated by autolysin, provides the important component of biofilm matrix, and suggests an additional role for autolysin in biofilm formation (Bose *et al*., 2012). AtlA also interacts with multiple human extracellular proteins, which promotes host colonization and contributes to *S. aureus* pathogenesis. An AtlA mutant strain shows higher cell aggregation, reduced biofilm formation, decrease binding with host matrix proteins and resistance to lyse in the presence of Triton X-100 (Bose *et al*., 2012; Komatsuzawa *et al*., 1997; Takahashi *et al*., 2002). The *sprX* knockdown strain in our study exhibited, in addition to reduced autolysin, a significant down-regulation of biofilm formation, high cell clustering phenotype and resistance to lysis, all of which confirm to down-regulation of autolysin expression.

4.9 SprX regulates the genes involved in cell wall metabolism in *S. aureus* Newman

Autolytic activity is a complex regulatory process and controlled by various pleiotropic regulators including the WalKR (aka YycGF), an important two-component regulator of autolysins including AtlA, IsaA, and LytM in *S. aureus*. Since *sprX* knockdown influenced multiple autolysins in cells, it seemed likely that SprX might regulate a common regulator of autolysins.

The effect of modified levels of SprX on the expression of the autolysin regulator *walR*, and selected autolysins *atlA* and *lytM*, all of which harbored a WalR box**,** was analyzed by qRT-PCR at different time points along the growth (Figure 21). In the cases of both, control and overexpression strains, a 3-4- fold higher expression of the *walR*, *atlA* and

lytM mRNAs was recorded at the exponential phase compared to the stationary phase, as seen in Figure 21, (A, B and C) and as has been reported (Dubrac *et al*., 2007; Oshida *et al*., 1998; Singh *et al*., 2010). Significant down regulation of *walR* transcripts to 0.2-0.4 fold, and of the two autolysins *altA* and *lytM* to 0.1-0.2 fold, was seen in the *sprX* knockdown strain compared to the control (Figure 21).

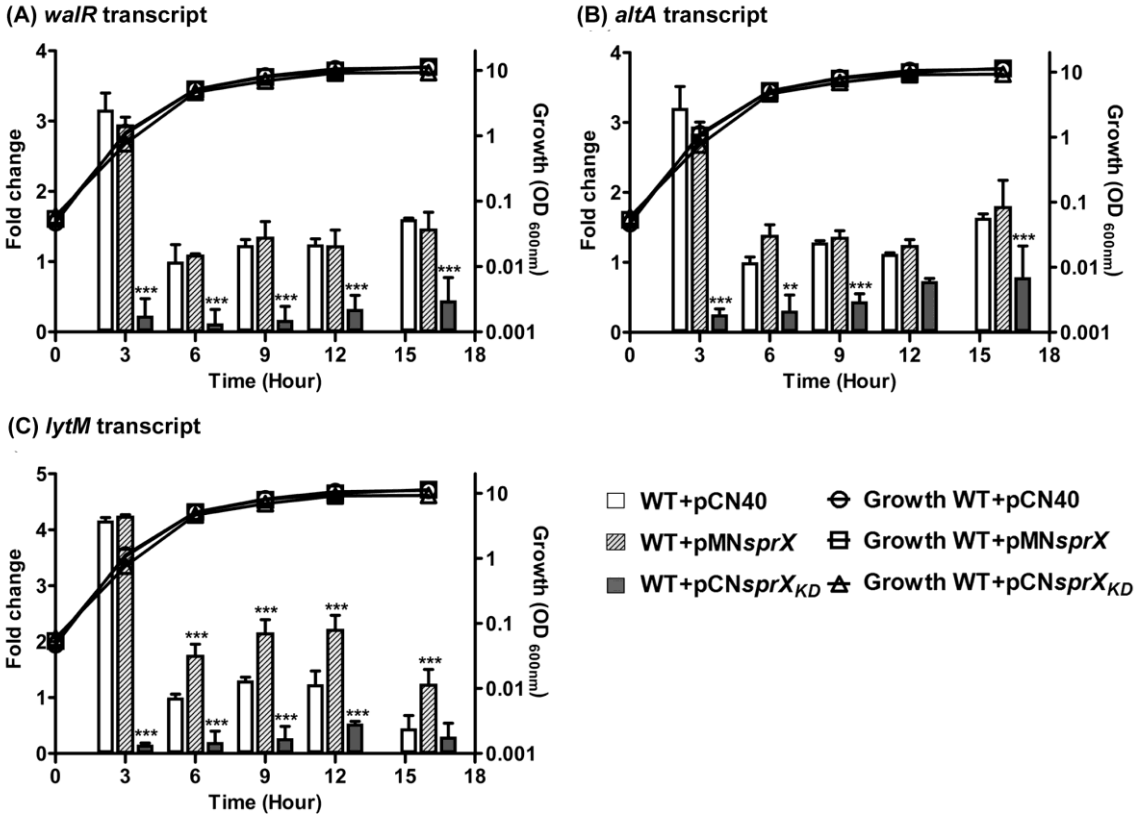

Figure 21: Influence of SprX levels on the expression of *walR*, *atlA*, and *lytM* transcripts in *S. aureus* Newman

Expression of *walR* (A), *atlA* (B), and *lytM* (C) in control (WT + pCN40), overexpression (WT + pMN*sprX*) and knockdown (WT + pCN$sprX_{KD}$) strains of *S. aureus* Newman, analyzed along the growth time by qRT-PCR. Values were normalized against 5S rRNA and fold change in expression was determined by the standard ΔΔCt method referred to the control (WT + pCN40) at 6 h of growth. Significant down regulation of *walR* (0.2-0.4 fold), *atlA* (0.2 fold), and *lytM* (0.1 fold) transcripts were revealed in *sprX* knockdown strain compared to the control. Differential expression of *lytM* transcripts is seen under *sprX* overexpression. Mean and standard deviation of triplicates are plotted. * represents the statistically significant difference analyzed by two-way ANOVA and each time point compared with control. *** (P<0.001), ** (P<0.01) and * (P < 0.05).

Overexpression of SprX did not influence the levels of *walR* RNA but resulted in a differential regulation of *lytM* mRNA. An overall significant up regulation of *lytM* by 1.2

- 2.2 fold (Figure 21C) was observed in *sprX* overexpression strain compared to the control.

Regulated expression of autolysin and peptidoglycan remodeling are essential for cell viability and division, and is involved in pathogenicity of *S. aureus*. WalK (histidine kinase) / WalR (response regulator) is a highly conserved two-component system among low GC Gram-positive bacteria. The WalKR positively regulates the autolysin expression, biofilm formation, promotes the host inflammatory response and plays an important role in *S. aureus* virulence (Delauné *et al*., 2012).

WalR recognizes and binds to the tandem repeated hexanucleotide with a spacer of five nucleotides [5′-TGT(A/T)A(A/T/C)-N_5-TGT(A/T)A(A/T/C)-3′] and control the expression of genes involved in cell wall metabolism (Dubrac *et al*., 2007; Dubrac and Msadek, 2008, 2004). In our analysis, the genes encoding autolysins AtlA, LytM, IsaA were found to have WalR protein interaction sequence, upstream the promoter region. Expression of WalR is regulated by two σ^A promoters which are found in many housekeeping genes and higher expression is reported at exponential growth phase (Arbade, 2016; Phanaksri *et al*., 2015). This corroborates with our observation of higher expression of *walR* and its downstream genes *atlA, lytM* in exponential phase.

WalR binding site was predicted around 54 nucleotides upstream to the transcription start site of AtlA. A six- fold and two- fold increase respectively in *atlA* (Figure 21) and *isaA* (Figure 15) expressions were reported with induction of WalR, further suggesting that transcription activation with respect to each gene varies due to variation of consensus promoter sequence and positioning of WalR binding site (Dubrac *et al*., 2007).

4.10 SprX interacts with WalR, a positive regulator of autolysin

Above results on the down regulation of autolysins in zymography, physiological assays and transcriptional analyses in *sprX* knockdown strain guided further investigation on the interaction between sRNA SprX and mRNAs of regulator WalR. *In silico* RNA-RNA interaction between sRNA SprX and *walR* mRNA analyzed using IntaRNA program revealed base pairing between 5′coding region of *walR* mRNA (U8 to A38) with loop 1 and 2 of SprX from A3 to U30 nt (Figure 22).

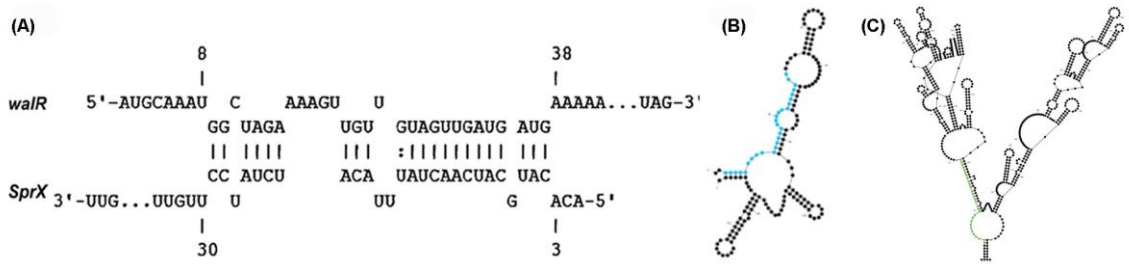

Figure 22: *In silico* analysis of mRNA-sRNA interaction

(A) IntaRNA analysis showing predicted interactions of SprX with *walR* mRNA. (B) Secondary structure of SprX predicted with Mfold. Region of SprX that base pairs with *walR* mRNA (A3-U30 nucleotides) is highlighted as blue. (C) Secondary structure *walR* mRNA and region that interact with SprX (U8-A38 nucleotides) is highlighted as green.

The above potential interaction for regulation of *walR* by SprX was analyzed by *in vitro* RNA-RNA interaction by gel mobility shift assays. *sprX* and *walR* transcripts containing the predicted interaction regions were *in vitro* transcribed, gel-purified and incubated with increasing molar ratios of DIG-labeled SprX. A strong complex formation between SprX and *walR* mRNA was detected in the presence of excess molar ratio of WalR in the range of 4-40 pmol (Figure 23A). At an increasing concentration of WalR, SprX was cleared to form an increased amount of complex (Figure 23A & B). The specificity of SprX-*walR* mRNA interaction was demonstrated by a competition assay in presence of 10-20- fold molar excess of nonspecific RNA PhrD (small RNA of *Pseudomonas aeruginosa* transcribed from a cloned plasmid) as well as 10 to 500-fold molar excess of unlabeled SprX (Figure 23C). The complex formation between SprX-*walR* mRNA was not displaced at a 20-fold excess molar ratio of the non-specific RNA PhrD. The addition of excess of unlabeled SprX beyond 50x, diminished the signal strength of complex formed. These results indicate that SprX directly interacts with *walR* mRNA. The strong interaction of *walR* mRNA (regulator of IsaA) with SprX *in vitro* shows that SprX influences the expression of IsaA and other autolysins via WalR, by directly interacting with *walR* mRNA.

4.11 Role of SprX in the complex network of regulation of autolysins

The direct interaction of SprX with *walR* mRNA and its effects observed on the expression of downstream genes of *walR* regulon endorses SprX as a significant regulator of autolysins in *S. aureus*. The down-regulation of *isaA* to 0.6-0.9 fold, seen unlike in

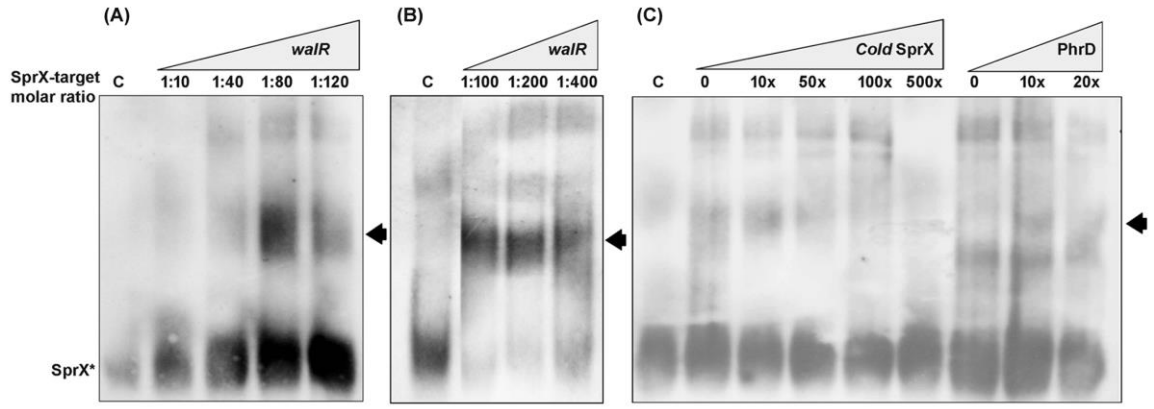

Figure 23: Interaction of SprX with *walR* mRNAs by gel mobility shift assay

DIG-labeled SprX was incubated with increasing concentrations of unlabeled mRNAs. Complex was resolved on 6% native-PAGE followed by transfer to Nylon membrane and detection by anti-DIG antibody (A) and (B) 0.1 pmol of SprX incubated with increasing molar ratio, 10x- 400x (1- 40 pmol) of WalR, showing depletion and clearance of substrate at higher ratios. The two gels are from independent experiments and have a difference in loading intensity (C) Specificity of SprX-*walR* mRNA interaction, analyzed in presence of competitor RNA PhrD (10x-20x) and cold (unlabeled) SprX (10-500x). SprX:WalR ratio (1:80) is kept constant in all the lanes. Black arrow represents SprX-*walR* complex.

other autolysins, under *sprX* overexpression in our experiments (Figure 15) can be elaborated by considering its complex multifactorial regulation (Figures 24 and 25). Most importantly, the interaction of SprX at the 3′ coding region of *isaA* mRNA (Figure 24A) may negatively influence its stability, a possibility that does not exist with other three autolysins tested. Although IsaA is positively and independently regulated by WalKR (YycGF), SarA and SrrAB (Melanie R Stapleton *et al*., 2007), it is also negatively regulated by another sRNA, RNAIII (Dunman *et al*., 2001), which in turn is positively regulated by SprX (Figure 25). SprX may interact at the 5' region of RNAIII, encoding the delta hemolysin, which further releases the intra molecular base pairing between 5' and 3' end and stabilizes RNAIII (Kathirvel *et al*., 2016). Cell wall associated proteins are generally repressed in the late exponential phase by *agr* system, mainly through RNAIII, which is expressed from the *agr* locus (Sakata and Mukai, 2007).

RNAIII regulates the expression of various cell wall associated proteins including IsaA, SceD, LytM (Bronesky *et al*., 2016). Base pair interaction was predicted between the C-rich motif at the 3′ domain of RNAIII and the region of ribosome binding site of mRNAs encoding proteins involved in cell wall metabolism [IsaA (Figure 24A), SceD, LytM, SsaA] (Lioliou *et al*., 2016), and was experimentally demonstrated for LytM. This

Figure 24: Schematic illustration of regulation at the nucleotide sequence of *isaA* and *lytM* genes
(A) The upstream promoter region of *isaA*: The two WalR binding sites (-152 to -137, -133 to -100) are indicated in blue; the conserved direct repeats are marked with an arrow. The putative 7 bp SarA binding region (-90 to -84) is in green (boxed). The RNAIII interacting region (+12 to +47) covers the ribosome binding site (RBS), +23 to +28 (boxed). SprX interacts at the 3′ end of coding region (+707 to +731), indicated as green fonts, and boxed. (B) The upstream region of *lytM*: The WalR binding region (-116 to -80, bold fonts). Conserved direct repeats are marked by an arrow. The RNAIII interaction region (+33 to +58) includes RBS (+34 to +39) and is boxed. RBS, -35 and -10 promoter regions are red and underlined. The nucleotide positions indicated are relative to the transcriptional start site.

suggested that RNAIII negatively regulates the expression of genes involved in cell wall metabolism at the late exponential to stationary phase, and WalR positively regulates their expression during the exponential phase. Further the two WalR binding stretches in *isaA* at -189 to -173 and -170 to -136 (Dubrac and Msadek, 2004) are followed by a 7 bp SarA binding region immediately downstream, as reported for *Staphylococcus* strain 2PF-18 (Sakata and Mukai, 2007). Thus, SarA binding may interfere with the expression of *isaA* transcripts under WalR regulation (Figure 24A). Thus the influence of SprX, indirectly mediated via RNAIII, and directly exerted on IsaA (Kathirvel *et al.*, 2016), together with the inhibition of WalR binding by SarA might account for the differential regulation of IsaA.

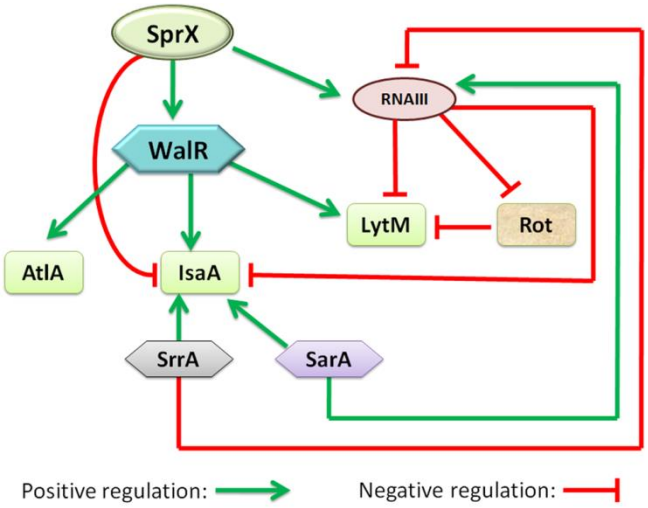

Figure 25: Regulatory network of SprX in autolysin regulation in *S. aureus.*
SprX positively influences the WalR expression and in turn regulates the expression of AtlA, IsaA, and LytM. Besides, SprX directly coordinates the expression of IsaA and RNAIII. The expression of IsaA and LytM is additionally controlled by different regulators (SrrA, SarA, RNAIII, Rot), which indicates that their regulation is complex and multifactorial. These represent the importance of small RNA SprX in autolysin regulation and fitness in *S. aureus*. Positive regulation is indicated by green arrow and negative regulation by red bar.

In contrast to *atlA* mRNA, *lytM* mRNA showed a marked increase under *sprX* overexpression in our studies that can be explained by its regulation under multiple regulators (Figure 24B). WalR directly binds to the region of *lytM* at -116 to -80, with respect to the transcriptional start site, and positively influences its expression during exponential growth phase (Dubrac and Msadek, 2004; Lioliou *et al.*, 2016). In addition to

WalR and RNAIII, the expression of *lytM* is also negatively regulated at the promoter by the pleiotropic transcriptional regulator Rot (Chu *et al*., 2013). RNAIII also represses the translation of *rot* by base pairing at two different regions including the ribosome binding site, and indirectly regulates the expression of various exoproteins (Chunhua *et al*., 2012). These remarkable multiple levels of regulation of the genes encoding autolysins and virulence determinants suggest that expression of each of these factors requires to be specifically controlled during the infection (Figure 25). The regulation of cell wall hydrolyzing autolysins by sRNA SprX, in addition to its involvement in the expression of other virulence factors of *S. aureus*, demonstrate a fine tuning in the expression of several virulence determinants where in SprX adds another layer of regulation by coordinating the expression of genes involved in cell wall metabolism and virulence.